

## Direct Observation of Surface-Mediated Electron–Hole Pair Recombination in TiO<sub>2</sub>(110)

Zhen Zhang and John T. Yates, Jr.\*

Department of Chemistry, University of Virginia, Charlottesville, Virginia 22904

Received: October 31, 2009; Revised Manuscript Received: January 15, 2010

The kinetics of surface and bulk electron–hole pair recombination have been measured separately on TiO<sub>2</sub>(110) in ultrahigh vacuum under well-controlled surface conditions for the first time. Using 100 eV incident electrons, excitation of electron–hole pairs occurs within  $\sim 6$  Å of the surface, and the rate of stimulated desorption of O<sub>2</sub> was measured as a means of determining the charge carrier recombination kinetics, which are found to be mediated by the surface and to be first-order in charge carrier concentration. Comparison with a previous O<sub>2</sub> photodesorption experiment, where excitation by 3.4 eV photons was used for electron–hole pair generation in a deeper region below the surface ( $\sim 100$  Å), shows that bulk recombination in TiO<sub>2</sub> occurs by second-order kinetics in charge carrier concentration.

Titanium dioxide (TiO<sub>2</sub>) has wide and important applications in the fields of photoelectronics and photocatalysis,<sup>1–5</sup> making it one of the most studied metal oxides in surface science. Two reactions occur in the photocatalytic process,<sup>2</sup> one being the oxidation reaction by the photogenerated holes and the other the reduction reaction by photogenerated electrons. The concentration of photogenerated carriers (electrons and holes) is important in determining photocatalysis efficiency. In the past few years, great efforts have been exerted to study the behavior of the photogenerated charge carriers in TiO<sub>2</sub> by studies of carrier generation and transport, carrier recombination, and carrier induced chemical reactions.<sup>1–6</sup>

There are three basic recombination mechanisms that are responsible for carrier annihilation in a semiconductor:<sup>7</sup> (1) band-to-band recombination, which occurs when an electron moves from the conduction band (CB) to the empty valence band (VB) containing a hole [the rate of band-to-band recombination depends on the product of the concentrations of available electrons and holes and is second order in charge carrier concentration];<sup>7</sup> (2) trap-assisted recombination (Shockley–Read–Hall Model, SRH model),<sup>7–9</sup> which occurs when an electron in the CB recombines indirectly with a hole in the VB at a “trap” state; and (3) Auger recombination, which occurs when an electron–hole pair recombine in a band-to-band transition giving off the generated energy to another electron or hole.<sup>7</sup>

The role of electron–hole recombination processes at the surface of TiO<sub>2</sub> has been investigated in a number of studies of TiO<sub>2</sub> colloidal particles.<sup>10–15</sup> These studies have generally shown that there are particle sizes of TiO<sub>2</sub> with optimized photocatalytic activity. Optimization occurs as detrimental surface-recombination effects on small particles are balanced by enhanced surface-active area effects. Measurements on colloidal semiconductor particles are influenced by solvent effects, adsorption effects, pH effects, and grain-to-grain charge transfer effects. Both photocatalytic activity<sup>10,14</sup> and photoluminescence<sup>11–13</sup> have been used to probe surface and bulk recombination in TiO<sub>2</sub>. In ZnO,<sup>16</sup> EPR was used to measure the optimization of photogenerated hydroxyl radicals on powdered material. There are no studies

of single-crystal TiO<sub>2</sub> where surface and bulk recombination effects have been separated under conditions of well-controlled surface composition and structure.

Surface science methodology offers great opportunities for the study of the electron–hole recombination processes. Using O<sub>2</sub> as a probe molecule, Thompson and Yates<sup>17–19</sup> found that adsorbed O<sub>2</sub> on TiO<sub>2</sub>(110) at 110 K can be stimulated to desorb by photogenerated holes and the rate of O<sub>2</sub> photodesorption increased with the square root of the photon flux. This indicates that the electron–hole (e–h) recombination in photoexcited TiO<sub>2</sub> occurs through a second-order kinetic mechanism. Kimmel et al.<sup>20,21</sup> found that electron-stimulated O<sub>2</sub> desorption occurs from the TiO<sub>2</sub>(110) surface. In this paper, we compare the kinetics of electron–hole recombination, when electrons and photons are separately used for excitation. O<sub>2</sub> desorption was used as a monitor of the charge carrier recombination kinetics.

The experiments were performed in an ultrahigh vacuum chamber with a base pressure of  $2 \times 10^{-11}$  mbar.<sup>22</sup> The TiO<sub>2</sub>(110) single-crystal (Princeton Scientific, 7 mm  $\times$  7 mm  $\times$  1 mm) was mounted on a tantalum support plate with a high-temperature alumina-based inorganic adhesive (Aremco 503). Two tungsten wires were spot-welded at the back of the Ta plate for resistive heating. The temperature of the crystal was measured and electronically controlled with a K-type thermocouple contacting the back of the TiO<sub>2</sub> crystal through a hole in the tantalum support. The TiO<sub>2</sub>(110) crystal was cleaned by Ar<sup>+</sup> sputtering followed by annealing at 900 K in vacuum. Within the sensitivity limits of Auger spectroscopy, the surface was free of contamination. Low-energy electron-diffraction (LEED) measurements on the cleaned surface showed a sharp (1  $\times$  1) pattern. This preparation procedure reproducibly yields a TiO<sub>2</sub>(110) surface with about 8–10% bridge-bonded oxygen (BBO) vacancies which are active for O<sub>2</sub> adsorption. Adsorption of <sup>18</sup>O<sub>2</sub> (99% isotopically pure) was carried out with use of a calibrated capillary array doser.<sup>23</sup> For the electron-stimulated desorption (ESD) experiment, a 100 eV electron beam was produced by an electron gun (Kimball Physics ELG-2) and the desorption of O<sub>2</sub> was detected by a line-of-sight quadrupole mass spectrometer (QMS) (UTI-100C) monitoring the <sup>18</sup>O<sub>2</sub><sup>+</sup> mass spectrometric signal. The electron flux was controlled by tuning the electron gun parameters and was measured by a picoammeter

\* To whom correspondence should be addressed. E-mail: johnt@virginia.edu.

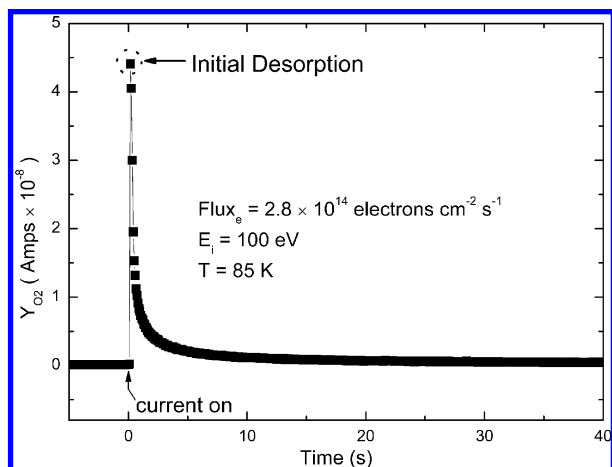


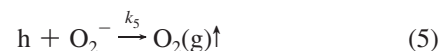
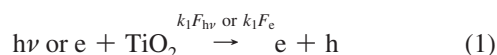
**Figure 1.** Electron stimulated desorption measurement for <sup>18</sup>O<sub>2</sub> on TiO<sub>2</sub>(110) surface using QMS. <sup>18</sup>O<sub>2</sub> is adsorbed to saturation coverage at 85 K.

(Keithley 6487) with +10 V biasing at the sample to suppress the secondary electron emission.

Figure 1 shows a typical electron stimulated desorption measurement of <sup>18</sup>O<sub>2</sub> on a TiO<sub>2</sub>(110) surface at an electron flux of  $2.8 \times 10^{14}$  electron  $\text{cm}^{-2} \text{s}^{-1}$ . Similar to O<sub>2</sub> photodesorption on the TiO<sub>2</sub>(110) surface,<sup>17,18</sup> the <sup>18</sup>O<sub>2</sub> signal reached a maximum within  $\sim 0.2$  s (indicated by the dashed circle) of the time when the electron current is established and then monotonically decreases over time as the chemisorbed <sup>18</sup>O<sub>2</sub> is depleted by the electron-stimulated desorption. A detailed analysis of the Y<sub>O<sub>2</sub></sub> decay kinetics shows that many decay constants are needed to fit the curve, as previously found for O<sub>2</sub> photodesorption.<sup>19</sup> The absence of single first-order kinetics in the O<sub>2</sub> depletion process indicates that a simple model involving O<sub>2</sub> direct excitation would be incorrect and that substrate-mediated kinetics apply, which will be discussed below. As discussed in ref 18, the O<sub>2</sub>-QMS signal is directly proportional to the rate of O<sub>2</sub> desorption ( $-d[\text{O}_2(\text{a})]/dt$ ), because the kinetics for O<sub>2</sub>(a) desorption from the surface are slow compared to the mass spectrometer pumping speed in the rapidly pumped vacuum system. So, the initial maximum <sup>18</sup>O<sub>2</sub> QMS signal represents the initial <sup>18</sup>O<sub>2</sub> electron stimulated desorption rate at the initial saturation coverage of <sup>18</sup>O<sub>2</sub> on the BBO vacancy sites.

The variation of the initial <sup>18</sup>O<sub>2</sub>(a) stimulated desorption rate has been measured as shown in Figure 2a as a function of electron flux for identical <sup>18</sup>O<sub>2</sub> coverages. The initial <sup>18</sup>O<sub>2</sub> desorption rate is linearly proportional to the electron flux ( $F_e$ ). In Figure 2b, where photon-stimulated desorption is measured, two separate O<sub>2</sub> desorption processes have been found: one is characteristic of low photon fluxes (branch A) and the second is characteristic of high photon fluxes (branch B). Both the slow and fast O<sub>2</sub> photodesorption processes are described by a rate law that is proportional to the square root of the incident photon flux ( $F_{\text{hv}}^{1/2}$ ).

Previous experiments<sup>4,17–19,24,25</sup> and theoretical calculations<sup>26</sup> suggest that the O<sub>2</sub> photodesorption is caused by the capture of a photogenerated hole. A kinetic scheme describing the elementary steps of e-h pair generation (step 1), hole and electron trapping at trap states (steps 2 and 3), e-h direct recombination (step 4), and O<sub>2</sub>(a) desorption by holes (step 5) is shown below:



For step 5, the O<sub>2</sub> desorption rate is  $-d[\text{O}_2^-(\text{a})]/dt = k_5[\text{O}_2^-(\text{a})][h]$ . Therefore, the O<sub>2</sub> desorption rate in Figure 2a is governed by the relationship of hole concentration ([h]) to the incident electron flux under conditions of constant O<sub>2</sub> coverage.

In the UV photon-excited experiment (Figure 2b), the hole concentration is a linear function of the square root of photon flux ( $F_{\text{hv}}^{1/2}$ ), which is characteristic of a band-to-band recombination mechanism. As discussed in ref 18, the photons excite electrons from the VB to the CB and produce the same concentration of electrons in the VB and holes in the CB (step 1). A fast equilibrium is established between the e-h pair generation (step 1) and recombination (step 4). From the steady state approximation, the hole concentration ([h]) should be a constant during the photon-excited experiment ( $d[h]/dt = k_1 F_{\text{hv}} - k_4[h][e] = 0$ ) (here step 2 is assumed to be negligible.). Then the concentration of holes [h] is

$$[h] = \left[ \frac{k_1}{k_4} \right]^{1/2} F_{\text{hv}}^{1/2} \quad (6)$$

and the O<sub>2</sub> desorption rate is

$$-d[\text{O}_2^-(\text{a})]/dt = k_5[\text{O}_2^-(\text{a})] \left[ \frac{k_1}{k_4} \right]^{1/2} F_{\text{hv}}^{1/2} \quad (7)$$

which agrees well with the experimental results that the O<sub>2</sub> desorption rate is proportional to the square root of the photon flux ( $F_{\text{hv}}^{1/2}$ ) as shown clearly in branch B in Figure 2b. The slower part (branch A) in Figure 2b is due to the trap filling process (step 2) at low photon fluxes.<sup>18</sup>

But the above band-to-band recombination mechanism does not fit the electron excited experiment. From Figure 2a, the O<sub>2</sub> desorption rate is proportional to the first power of the electron flux ( $F_e$ ), indicating the hole depletion follows *first-order recombination kinetics*, which usually happens in the SRH recombination mechanism. The main path for the hole depletion is capture by hole traps as indicated in step 2 in the electron-excited experiment instead of the recombination with the hole directly (step 4) as in the photon experiment. For the steady state approximation,  $d[h]/dt = k_1 F_e - k_2[h][T] = 0$ , or  $[h] = k_1 F_e / k_2 [T]$ , and

$$-d[\text{O}_2^-(\text{a})]/dt = k_5[\text{O}_2^-(\text{a})] \left[ \frac{k_1}{k_2} \right] \frac{F_e}{[T]} \quad (8)$$

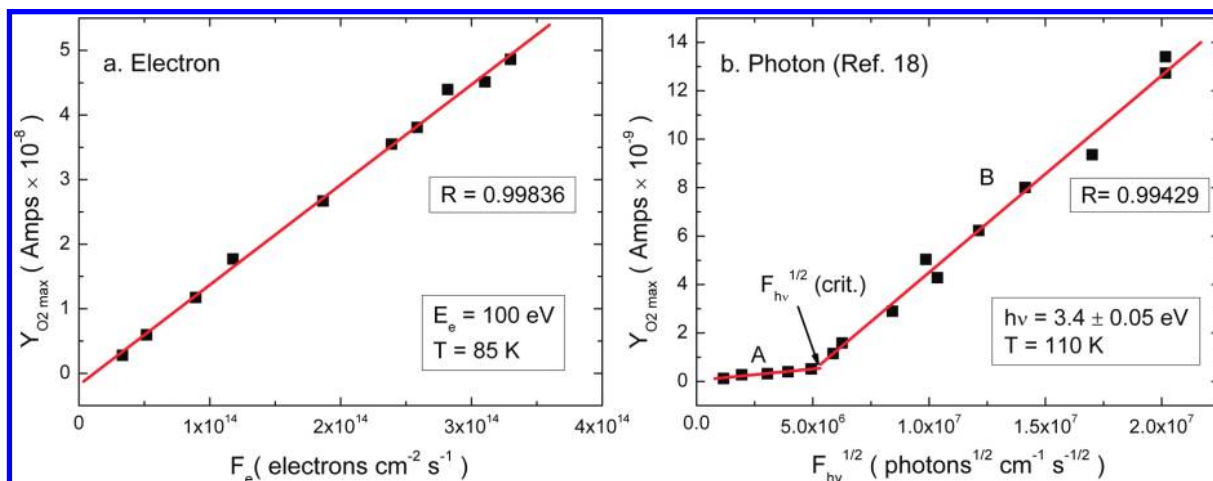


**Figure 2.** Plots showing the initial photodesorption yields of  $^{18}\text{O}_2$  from  $\text{TiO}_2(110)$  as a function of (a) incident electron flux ( $F_e$ ) and (b) the square root of the incident UV photon flux ( $F_{\text{hv}}^{1/2}$ ).

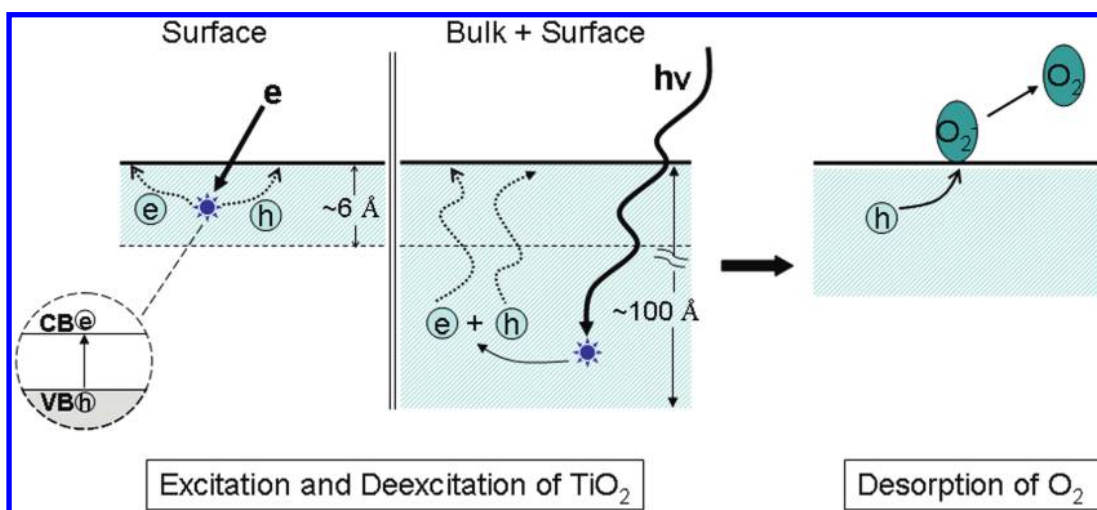


**Figure 3.** Schematic electron and photon excitation processes in  $\text{TiO}_2$  followed by deexcitation events. In the electron-excitation, the near-surface electrons and holes quickly diffuse to the surface traps and recombine there by first-order kinetics by the Shockley–Read–Hall mechanism. In the photon-excitation, the bulk electrons and holes will recombine directly in the bulk by second-order kinetics. Some of the holes are captured by  $\text{O}_2^-$  (a) causing  $\text{O}_2$  desorption for both electron and photon excitation.

If we assume the hole trap concentration ( $[T]$ ) is constant, then  $[h]$  is proportional to the electron flux, which agrees with the experimental result where first-order kinetics are observed.

The different mechanism of electron–hole recombination in the electron- and photon-excited experiment is due to the different absorption lengths for the incident electrons and photons in the  $\text{TiO}_2$ . As indicated in Figure 3, electrons and UV photons exhibit a large difference in excitation depth. The electron inelastic mean free path for 100 eV electrons in  $\text{TiO}_2$  solid is estimated to be  $\sim 5.6 \text{ \AA}$  (2–3 atomic layer depth) according to the TPP-2M equation,<sup>27</sup> while the UV (3.4 eV) absorption length is  $\sim 103 \text{ \AA}$ .<sup>18</sup> Therefore, electrons and holes excited by *electron impact* are produced in the near surface region, while *photons* penetrate deeper into the bulk region producing more bulk electron–hole pairs. In the near surface region of the  $\text{TiO}_2$  crystal, there exists a large concentration of surface defects, such as step edges, oxygen vacancies, line defects, impurities, and Ti interstitials, which may act as trap sites for the electron–hole recombination by the SRH mechanism. In addition, the surface Ti and O atoms may also be carrier traps due to the unsaturated coordination caused by the broken symmetry in the surface. The electron-produced holes near the surface can therefore be quickly captured by the surface traps (step 2), then recombining promptly by first-order kinetics with

electrons at the surface traps (step 3). In contrast, for the photon-excited experiment, most of the generated electrons and holes directly recombine by second-order kinetics through the band-to-band recombination due to the presence of fewer defects in the bulk.

In the photon experiment, we also notice a slow  $\text{O}_2$  photo-desorption process occurring in the low photon flux region (below  $F_{\text{hv}}(\text{crit.})$  in branch A of Figure 2b). This is due to the filling process of the bulk-hole traps in the  $\text{TiO}_2$  crystal, which also indicates the bulk-hole trap concentration is small compared with the concentration of photogenerated holes in this experiment. In the electron experiment, the low desorption rate process has not been found, which agrees with our assumption that the trap concentration  $[T]$  at the  $\text{TiO}_2$  surface is large. There are two possible reasons for the constant hole-trap concentration. One is the huge concentration of the surface trap sites compared with the electron-produced holes, so the hole concentration variation over a range of incident electron fluxes cannot significantly influence the trap density. A second possibility is that the large flux of incident electrons may influence the kinetic order (in electrons) of the desorption process. In the electron-excited experiment, the incident electrons lose their energy and finally reside at the CB. The huge concentration of incident- and electron-produced secondary electrons will quickly recom-

bine with the hole-filled traps (step 3) and regenerate the trapping holes, thus keeping the hole-trap concentration constant.

One may argue that the interpretation could be modified if extensive band bending occurs in the near surface region of the TiO<sub>2</sub>(110) causing modification of the kinetics of e-h recombination. When the O<sub>2</sub> was exposed to the TiO<sub>2</sub> surface, some of the defects were filled by the oxygen and the oxygen is negatively charged, which forms a reverse electric field and compensates the band bending of the clean TiO<sub>2</sub> surface.<sup>1,28</sup> Thus the degree of band bending will be minimized by O<sub>2</sub> adsorption. Furthermore, band bending would be expected to occur over a large depth of order of hundreds of Ångströms,<sup>29</sup> and would therefore affect both the electron and photon excited process. Therefore it is unlikely that band bending will be responsible for the different observed kinetics of O<sub>2</sub> stimulated desorption by electrons and photons.

In summary, the electronically stimulated desorption of O<sub>2</sub> has been used as a probe to determine the hole depletion kinetics for electron- and photon-excitation of TiO<sub>2</sub>, and a different hole depletion mechanism has been discovered for electron excitation compared to photon excitation. Figure 3 shows the schematic electron- and photon-excitation processes in TiO<sub>2</sub> followed by the deexcitation events. For the electron-excitation, the electrons and holes which are produced mainly in the near surface region will quickly diffuse to the surface traps and then annihilate in the traps (SRH mechanism). The electron–hole recombination by surface trap sites follows first-order kinetics. For the photon-excitation, the electrons and holes will be produced mainly deep in the bulk. Due to the presence of fewer defects in the bulk, the electron–hole pairs recombine in the bulk following second-order e-h recombination kinetics.

**Acknowledgment.** We acknowledge with thanks the support of this work by the Defense Threat Reduction Agency (DTRA) under contract HDTRA-07-C0085.

## References and Notes

- (1) Diebold, U. *Surf. Sci. Rep.* **2003**, *48*, 53.
- (2) Fujishima, A.; Zhang, X. T.; Tryk, D. A. *Surf. Sci. Rep.* **2008**, *63*, 515.

- (3) Linsebigler, A. L.; Lu, G. Q.; Yates, J. T., Jr. *Chem. Rev.* **1995**, *95*, 735.
- (4) Thompson, T. L.; Yates, J. T., Jr. *Chem. Rev.* **2006**, *106*, 4428.
- (5) Grätzel, M. *Nature* **2001**, *414*, 338.
- (6) Rubano, A.; Paparo, D.; Miletto, F.; di Uccio, U. S.; Marrucci, L. *Phys. Rev. B* **2007**, *76*, 125115.
- (7) Yu, P. Y.; Cardona, M. *Fundamentals of Semiconductors: Physics and Materials Properties*; Springer: New York, 2005.
- (8) Shockley, W.; Read, W. T. *Phys. Rev.* **1952**, *87*, 835.
- (9) Hall, R. N. *Phys. Rev.* **1952**, *87*, 387.
- (10) Zhang, Z. B.; Wang, C. C.; Zakaria, R.; Ying, J. Y. *J. Phys. Chem. B* **1998**, *102*, 10871.
- (11) Serpone, N.; Lawless, D.; Khairutdinov, R.; Pelizzetti, E. *J. Phys. Chem.* **1995**, *99*, 16655.
- (12) Cavigli, L.; Bogani, F.; Vinattieri, A.; Faso, V.; Baldi, G. *J. Appl. Phys.* **2009**, *106*, 053516.
- (13) Liu, B. S.; Zhao, X. J.; Wen, L. P. *Mater. Sci. Eng., B* **2006**, *134*, 27.
- (14) Liu, S.; Jaffrezic, N.; Guillard, C. *Appl. Surf. Sci.* **2008**, *255*, 2704.
- (15) Kopidakis, N.; Neale, N. R.; Zhu, K.; van de Lagemaat, J.; Frank, A. J. *J. Phys. Chem. Lett.* **2005**, *87*, 202106.
- (16) Dodd, A. C.; McKinley, A. J.; Saunders, M.; Tsuzuki, T. *J. Nanopart. Res.* **2006**, *8*, 43.
- (17) Lu, G. Q.; Linsebigler, A. L.; Yates, J. T., Jr. *J. Chem. Phys.* **1995**, *102*, 4657.
- (18) Thompson, T. L.; Yates, J. T., Jr. *J. Phys. Chem. B* **2005**, *109*, 18230.
- (19) Thompson, T. L.; Yates, J. T., Jr. *J. Phys. Chem. B* **2006**, *110*, 7431.
- (20) Kimmel, G. A.; Petrik, N. G. *Phys. Rev. Lett.* **2008**, *100*, 196102.
- (21) Petrik, N. G.; Zhang, Z. R.; Du, Y. G.; Dohnalek, Z.; Lyubinetsky, I.; Kimmel, G. A. *J. Phys. Chem. C* **2009**, *113*, 12407.
- (22) Lee, J.; Zhang, Z.; Yates, J. T., Jr. *Phys. Rev. B* **2009**, *79*, 081408.
- (23) Yates, J. T., Jr. *Experimental Innovations in Surface Science: A Guide to Practical Laboratory Methods and Instruments*; Springer: New York, 1998.
- (24) Sporleder, D.; Wilson, D. P.; White, M. G. *J. Phys. Chem. C* **2009**, *113*, 13180.
- (25) Perkins, C. L.; Henderson, M. A. *J. Phys. Chem. B* **2001**, *105*, 3856.
- (26) de Lara-Castells, M. P.; Krause, J. L. *J. Chem. Phys.* **2003**, *118*, 5098.
- (27) Tanuma, S.; Powell, C. J.; Penn, D. R. *Surf. Interface Anal.* **1993**, *21*, 165.
- (28) Hebenstreit, E. L. D.; Hebenstreit, W.; Geisler, H.; Thornburg, S. N.; Ventrice, C. A., Jr.; Hite, D. A.; Sprunger, P. T.; Diebold, U. *Phys. Rev. B* **2001**, *64*, 115418.
- (29) Zangwill, A. *Physics at Surfaces*; Cambridge University Press: Cambridge, UK, 1988.

JP910404E